

# Ethoxyquin mediates lung fibrosis and cellular immunity in BLM-CIA mice by inhibiting HSP90

Jie-Rou Huang<sup>1,2,A–D,F</sup>, Liang Chen<sup>3,B,E,F</sup>, Chao-Qian Li<sup>1,A,B,E,F</sup>

<sup>1</sup> Department of Respiratory Medicine, the First Affiliated Hospital of Guangxi Medical University, Nanning, China

<sup>2</sup> Department of Rheumatology and Immunology, Hunan Provincial People's Hospital, the First-Affiliated Hospital of Hunan Normal University, Changsha, China

<sup>3</sup> Department of Infectious Diseases, Hunan Provincial People's Hospital, the First-Affiliated Hospital of Hunan Normal University, Changsha, China

A – research concept and design; B – collection and/or assembly of data; C – data analysis and interpretation;

D – writing the article; E – critical revision of the article; F – final approval of the article

Advances in Clinical and Experimental Medicine, ISSN 1899–5276 (print), ISSN 2451–2680 (online)

*Adv Clin Exp Med.* 2025;34(2):211–225

## Address for correspondence

Chao-Qian Li

E-mail: lichaoqiangood@163.com

## Funding sources

This study was supported by Guangxi Natural Science Foundation (grant No. 2020GXNSFDA238003).

## Conflict of interest

None declared

Received on August 16, 2023

Reviewed on October 7, 2023

Accepted on March 22, 2024

Published online on September 16, 2024

## Cite as

Huang JR, Chen L, Li CQ. Ethoxyquin mediates lung fibrosis and cellular immunity in BLM-CIA mice by inhibiting HSP90. *Adv Clin Exp Med.* 2025;34(2):211–225. doi:10.17219/acem/186365

## DOI

10.17219/acem/186365

## Copyright

Copyright by Author(s)

This is an article distributed under the terms of the Creative Commons Attribution 3.0 Unported (CC BY 3.0) (<https://creativecommons.org/licenses/by/3.0/>)

## Abstract

**Background.** Patients with rheumatoid arthritis-associated interstitial lung disease (RA-ILD) are characterized by severe pulmonary fibrosis and immune dysregulation. Heat shock protein 90 (HSP90) is involved in the progression of pulmonary fibrosis and the immune response.

**Objectives.** This study aimed to explore whether HSP90 regulates the development of RA-ILD and its underlying mechanism.

**Materials and methods.** In vivo, collagen-induced arthritis (CIA)-mice were treated with bleomycin (BLM) to establish an arthritic mouse model of pulmonary fibrosis. In vitro, human lung fibroblast 1 (HLF1) was exposed to transforming growth factor beta 1 (TGF- $\beta$ 1) to simulate an RA-ILD model. The RA-ILD models were treated with the HSP90 inhibitor ethoxyquin (EQ) to explore the potential mechanism of HSP90 in RA-ILD. Histopathological analysis was performed, and pulmonary fibrosis was evaluated. The differentiation of M1/M2 macrophages and Th1/Th17/Treg cells was assessed. The role of the TGF- $\beta$ /Smad2/3 pathway in EQ-mediated RA-ILD progression was also explored.

**Results.** HSP90 $\alpha$  and HSP90 $\beta$  were upregulated in the RA-ILD models. Ethoxyquin mitigated arthritis in BLM-CIA mice, and reduced the expression of alpha-smooth muscle actin ( $\alpha$ -SMA), collagen I (Col-1) and fibronectin (FN), as well as hydroxyproline content, thereby relieving pulmonary fibrosis. In addition, EQ increased M1 macrophages and inducible nitric oxide synthase (iNOS) and tumor necrosis factor alpha (TNF- $\alpha$ ) levels; conversely, EQ decreased M2 macrophages and vascular endothelial growth factor (VEGF)-A and TGF- $\beta$ 1 contents. It also decreased Th17 (interleukin (IL)-17) while increasing Th1 (interferon gamma (IFN- $\gamma$ )) and Treg (Foxp3), and restricted the expression of transforming growth factor beta type receptor I and II (TGF- $\beta$ RI and TGF- $\beta$ RII) and the phosphorylation of Smad2 and Smad3.

**Conclusions.** This study revealed that EQ regulated pulmonary fibrosis and cellular immunity by inhibiting HSP90, appearing to act through the TGF- $\beta$ /Smad2/3 pathway. These findings suggest that EQ holds potential as a therapeutic agent for treating RA-ILD.

**Key words:** pulmonary fibrosis, HSP90, cellular immunity, rheumatoid arthritis-associated interstitial lung disease, ethoxyquin

## Background

Rheumatoid arthritis (RA) is a systemic autoimmune disease characterized by joint damage and inflammation.<sup>1</sup> It often also leads to the involvement of extra-articular organs, and one of the most common manifestations is interstitial lung disease (ILD), which affects more than 60% of RA patients. Unfortunately, the median survival time for patients with RA-associated ILD (RA-ILD) is only 3–7 years.<sup>2,3</sup> In addition to the dysregulated immune response, patients with RA-ILD develop irreversible lung fibrosis that resembles idiopathic pulmonary fibrosis.<sup>4,5</sup> While certain anti-fibrotic medications such as nintedanib and pirfenidone have shown promise as potential treatments for RA-ILD, some patients may require additional immunomodulatory therapy.<sup>6,7</sup> As a result, there is a pressing need to develop new treatment approaches that specifically target RA-ILD. This would significantly contribute to improving patients' overall health and quality of life.

T cell activation plays a crucial role in the pathology of pulmonary fibrosis.<sup>8</sup> T cells, which can be further categorized based on surface markers and cell functions, include natural killer T cells, CD8 cytotoxic T lymphocytes,  $\gamma\delta$  T cells, Treg (T regulatory, Foxp3) cells, and T helper cells. T helper cells can be further divided into different subsets such as Th1 (interferon gamma (IFN- $\gamma$ )), Th2 (interleukin (IL)-4), Th17 (IL-17), and Tfh (T follicular helper). Studies have shown that nintedanib, for instance, can regulate T cell activation and promote the release of IFN- $\gamma$ .<sup>9</sup> In the lungs of patients with RA-ILD, IL-17A is upregulated. This elevation of IL-17A stimulates the proliferation of fibroblast-like synoviocytes and the production of extracellular matrix (ECM) proteins.<sup>10</sup>

Macrophages are also present in the lungs of individuals with pulmonary fibrosis. Inflammatory responses typically lead to the activation of M1 macrophages by Th1 cells, while the Th2 cytokine IL-4 induces alternative activation of M2 macrophages (anti-inflammatory, pro-fibrotic).<sup>11,12</sup> Macrophages, acting as antigen-presenting cells, participate in T cell-mediated immune responses, and the activation of M1 or M2 macrophages can affect the occurrence of T cell responses.<sup>13</sup> Inhibition of M2 macrophage polarization has been reported to ameliorate the fibrotic phenotype of RA-ILD.<sup>14</sup> However, there is still a need to uncover more details about the various cellular immune states that exist in RA-ILD.

Heat shock protein 90 (HSP90) is a type of molecular chaperone protein involved in regulating protein balance, adaptive immune response, and cell differentiation and development.<sup>15</sup> In patients with pulmonary fibrosis, HSP90 has been reported to modulate collagen deposition and wound healing, increasing interest in the potential beneficial effect of HSP90 inhibition in pulmonary fibrosis.<sup>16</sup> Previous evidence has shown that citrullinated HSP90 (citHSP90) plays a significant role in immune response in RA-ILD. The citHSP90 stimulates T cells in RA-ILD to produce IFN- $\gamma$  in response to a Th1 response.<sup>17,18</sup> However, further confirmation

is needed to understand the precise role of HSP90 in the fibrotic and immune responses observed in RA-ILD.

Ethoxyquin (EQ) has long been used as an additive in animal feed to improve growth performance and disease resistance.<sup>19,20</sup> Due to its anti-inflammatory and antioxidant properties, EQ has shown potential in preventing acute liver injury and cancer.<sup>21,22</sup> Previous studies have illustrated the ability of EQ to decrease HSP90 activity, thereby alleviating peripheral axonal injury induced by chemotherapy and providing neuroprotection,<sup>23,24</sup> and suggesting the emergence of EQ as a potential inhibitor of HSP90. However, whether EQ can modulate RA-ILD progression by regulating HSP90 activity still needs to be elucidated.

The TGF- $\beta$ /Smad2/3 signaling pathway is widely recognized to mediate the process of pulmonary fibrosis.<sup>25,26</sup> Transforming growth factor-beta (TGF- $\beta$ ) drives the epithelial–mesenchymal transition (EMT) by activating the transcription factor involved in EMT (EMT-TF). The EMT is a crucial pathway for the formation of myofibroblasts, which are the central cells in pathological fibrosis.<sup>27,28</sup> Studies have found that microRNA-18-5p limited TGF- $\beta$ /Smad2/3 signaling and prevented the EMT of pleural mesothelial cells induced by bleomycin (BLM), ultimately alleviating subpleural lung fibrosis.<sup>29</sup> Vitamin D deficiency, on the other hand, leads to activation of the TGF- $\beta$ /Smad2/3 signaling and collagen deposition in the lungs, accelerating BLM-induced pulmonary fibrosis.<sup>26</sup> However, whether HSP90 mediates the TGF- $\beta$ /Smad2/3 signaling pathway to affect the progression of RA-ILD remains to be elucidated.

The establishment of the preventative models has helped to understand the role of EQ in RA-ILD. Arthritis and pulmonary fibrosis are 2 key pathological features of RA-ILD.<sup>30</sup> As an in vivo model, the collagen II (Col-2)-induced arthritis (CIA) model has been widely chosen for studying the pathogenesis of RA, as it is cost-effective and shares immunological and pathological features relatively similar to human RA.<sup>31,32</sup> Bleomycin is further used to induce animal pulmonary fibrosis and lung injury.<sup>33</sup> Additionally, TGF- $\beta$ 1 is activated in the process of pulmonary fibrosis. TGF- $\beta$ 1 predominantly drives lung fibroblast differentiation into myofibroblasts and stimulates excessive secretion of ECM proteins by myofibroblasts, leading to ECM deposition and fibrosis.<sup>34,35</sup> Therefore, the BLM-CIA mouse model and TGF- $\beta$ 1-induced human lung fibroblast 1 (HLF1) cell model were chosen to assess the effect of EQ on pulmonary fibrosis.

## Objectives

This study aims to generate a mouse model of RA-ILD, establish a TGF- $\beta$ 1-induced HLF1 cell model, and investigate the mechanism through which EQ affects the physiological and pathological phenotypes and immune cell characteristics associated with RA-ILD. These investigations will provide new insights for treating RA-ILD.

## Materials and methods

### Animal model

Male C57BL/6 mice (6–8 weeks old) were ordered from Hunan SJA Laboratory Animal Co., Ltd. (Changsha, China). Mice were randomly divided into 3 groups ( $n = 6$  in each group): sham, CIA+BLM and CIA+BLM+EQ. A brief flowchart of the animal model procedure is shown in Fig. 1. The CIA mice were treated with BLM to mimic the RA-ILD model as described previously.<sup>5,36</sup> The CIA was induced by Col-2 emulsified in Freund's complete adjuvant. On day 0, a subcutaneous injection of 100  $\mu$ L of emulsion containing 100  $\mu$ g of Col-2 and 200  $\mu$ g of *Mycobacterium tuberculosis* (Mtb) was administered at the base of the tail. On day 21, booster immunization was performed following the same procedure. On day 25, mice in the CIA+BLM and CIA+BLM+EQ groups were subjected to intrabronchial injections of 5 mg/kg BLM. On the same day, 8 h after BLM induction, mice in the CIA+BLM+EQ group were intraperitoneally injected with extra 0.36 mg/mouse EQ (E8260; Sigma Aldrich, St. Louis, USA).<sup>22</sup> From day 25 to day 45, mice received EQ 3 times a week for 3 weeks. The mice in the sham group received an equivalent dose of normal saline.

### Airway hyperresponsiveness analysis

A lung function challenge test was carried out the day following the final treatment administration. After the mouse was anesthetized and fixed, the skin of the neck was incised, and the trachea was bluntly dissected. After the trachea was exposed, sutures were used to pass through the trachea, the T-shaped entrance was opened in the trachea, and the endotracheal tube was inserted and then ligated and fixed. The airway responsiveness of the mice in each group was measured using a closed plethysmography system. The mice were sealed in a body scanning box, and after the baseline was stabilized, a bronchial challenge was performed with 0.5, 1, 2, 4, and 6 mmol/L methacholine (Mch) solutions (A2126; Sigma-Aldrich). At the end of each excitation, the 2<sup>nd</sup> excitation and detection were performed after the baseline stabilized. Changes in airway resistance parameters at different Mch concentrations were observed and calculated. Percentage reduction of lung compliance was calculated as

$$\frac{(\text{lung compliance value before challenge} - \text{lung compliance value after challenge})}{\text{lung compliance value before challenge}} \times 100\%.$$

### Tissue staining

Histopathological analysis was performed using hematoxylin and eosin (H&E) and Sirius red staining. Lung tissues were fixed in 4% paraformaldehyde. Joint tissues were fixed in 10% formalin and decalcified with ethylenediaminetetraacetic acid (EDTA). Paraffin embedding was performed on both lung and joint tissues, followed by sectioning into thin slices measuring 4–5  $\mu$ m. The extent of the damage in lung and synovial tissues was assessed using H&E staining. Collagen deposition in the synovium was assessed with Sirius red staining. Sections were deparaffinized with xylene and hydrated with alcohols of varying concentrations. Subsequently, sections were stained with H&E and Sirius red dye (Abiowell, Changsha, China). After dehydration, the sections were observed under an optical microscope (BA210T; Motic, Xiamen, China), and randomly selected fields of view were photographed.

### Immunohistochemistry staining

After deparaffinization and hydration, sections of the left lungs were heated in 0.01 mol/L citrate buffer for thermal antigen retrieval. To eliminate endogenous enzymes, 1% periodate was added. After washing with phosphate-buffered saline (PBS), the sections were incubated overnight at 4°C with alpha-smooth muscle actin ( $\alpha$ -SMA) antibody (1:300, BM0002; Boster, Wuhan, China). The next day, horseradish peroxidase (HRP)-labeled mouse antibody (1:100, AWS0003; Abiowell) was added. Briefly, 4',6-diamidino-2-phenylindole (DAPI) was chosen to stain nuclei, and hematoxylin was used to counterstain tissues. Finally, images were acquired under an optical microscope (BA210T; Motic) ( $\times 100$  and  $\times 400$  magnification) and analyzed with IPP (Image-Pro-Plus; Media Cybernetics, Rockville, USA).

### Flow cytometry

To assess the immune status of RA-ILD, peripheral blood and bronchoalveolar lavage fluid (BALF) were collected from the mice, and the proportion of immune cells was detected.

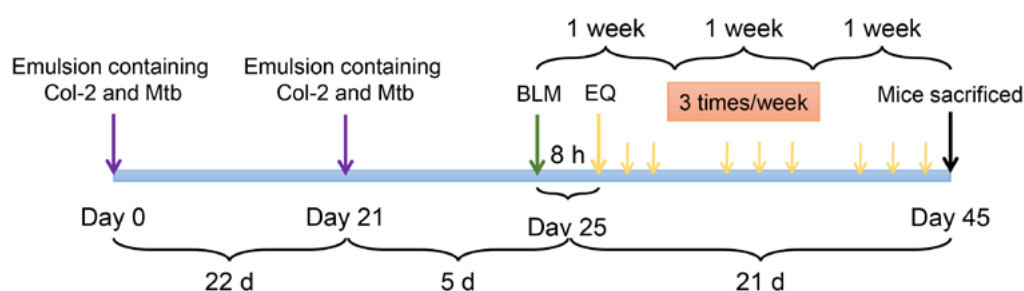


Fig. 1. Flowchart of the animal model procedure

Red cell lysate was added to fresh blood. After centrifugation, the cell pellet was suspended in PBS. Cells ( $1 \times 10^5$  cells/100  $\mu$ L) were washed with 0.01 M PBS (pH 7.4) and resuspended in the culture medium. Then, F4/80-FITC (11-4801-82; eBioscience, San Diego, USA) and CD11c-PE (12-0114-82; eBioscience) or F4/80-FITC and CD206-PE (12-2061-82; eBioscience) were added, and the cells were incubated in the dark for 30 min and washed with PBS. Subsequently, cells were analyzed for M1/M2 macrophage ratio with flow cytometry (A00-1-1102; Beckman Coulter, Fullerton, USA).

For Th1/Th17 detection, a cell stimulation cocktail was added to suspend cells. Cells were stimulated at 37°C for 4 h. After centrifugation, 0.5% bovine serum albumin (BSA)-PBS was added to wash the cells. Cells were suspended with intracellular fixation buffer and fixed at room temperature. Subsequently, cells were suspended with permeabilization buffer. CD4-FITC (11-0041-82; eBioscience) and IFN $\gamma$ -PE (12-7311-82; eBioscience) or CD4-FITC and IL17-PE (12-7177-81; eBioscience) were added and incubated for 30 min in the dark. Cells were washed with 0.5% BSA-PBS and analyzed using flow cytometry.

For Treg detection, cells were fixed and permeabilized. Subsequently, CD4-FITC, CD25-APC (17-0251-82; eBioscience) and Foxp3-PE (12-5773-82; eBioscience) were added, and the cells were incubated in the dark for 30 min. Cells were washed with 0.5% BSA-PBS and analyzed with flow cytometry.

## Enzyme-linked immunosorbent assay

Vascular endothelial growth factor (VEGF)-A, inducible nitric oxide synthase (iNOS), tumor necrosis factor alpha (TNF- $\alpha$ ), TGF- $\beta$ , IFN- $\gamma$ , IL-17, and Foxp3 levels in mouse serum and BALF were detected according to the kit instructions. VEGF-A (CSB-E04756m), iNOS (CSB-E08326m), TNF- $\alpha$  (CSB-E04741m), TGF- $\beta$  (CSB-E04726m), and IFN- $\gamma$  (CSB-E04578m) detection kits were ordered from Cusabio (Wuhan, China). The Foxp3 detection kit (YJ037859) was purchased from Yuanju Biological Co., Ltd. (Shanghai, China).

## Hydroxyproline detection

To quantify collagen metabolism, a hydroxyproline assay was performed according to the kit manual (A030-2-1; Nanjing Jiancheng Bioengineering Institute, Nanjing, China). The hydrolysate was added, and the tissue was hydrolyzed by heating in a water bath. The pH was adjusted to 6–6.8. The hydrolysate containing activated carbon was added and mixed well. The supernatant was collected after centrifugation, and the absorbance value of each tube was measured at 550 nm. The data show hydroxyproline content ( $\mu$ g per mg) of tissue.

## Quantitative real-time polymerase chain reaction

Total RNA was extracted from cell lysates and tissues using TRIzol (15596026CN; Thermo Fisher Scientific, Waltham, USA). RNA was then converted into cDNA using the HiFiScript cDNA Synthesis Kit (CW2569; CWBIO, Taizhou, China). The UltraSYBR mix kit (CW2601; CWBIO) was used to perform quantitative real-time polymerase chain reaction (qPCR) with the PCR system. The  $2^{-\Delta\Delta C_t}$  method was used to calculate the relative level of the target after  $\beta$ -actin standardization. The primer sequence is shown in Table 1.

## Western blot

Radioimmunoprecipitation assay (RIPA; AWB0136; Abiowell) was used to extract total protein from cell lysates or tissues, and then the protein concentration was quantified with a bicinchoninic acid (BCA) kit (AWB0104; Abiowell). Then, the total protein was separated using sodium dodecyl-sulfate polyacrylamide gel electrophoresis (SDS-PAGE) and transferred to a nitrocellulose (NC) membrane. The membrane was mixed with 5% skim milk powder and incubated for 90 min to prevent nonspecific binding. Subsequently, the membrane was incubated with

Table 1. Primer sequences used in the study

Targets	F (5'-3')	R (5'-3')
<i>M-TGF-<math>\beta</math>R</i>	AATTCCTCGAGACAGGCCATTT	CCAGCTGACTGCTTTTCTGTAG
<i>M-Smad2</i>	AATCATTGCAACAAGAGGCAGT	ATTCCTGCTCCCATCATCTT
<i>M-Smad3</i>	CCCTAGTCAAGCCAGTCCCT	AGCCTCCTAAACAAGAGTCCACACC
<i>M-IFN-<math>\gamma</math></i>	GCCACGGCACAGTCATTGA	TGCTGATGGCCTGATTGTCTT
<i>M-IL-17</i>	AGACTACCTCAACCGTTCCAC	CACCAGCATCTTCTCGACCC
<i>M-Foxp3</i>	CTCCAATCCCTGCCCTTGACC	ACATCATCGCCCGGTTTCCA
<i>M-<math>\beta</math>-actin</i>	ACATCCGTAAAGACCTCTATGCC	TACTCTGCTTGCTGATCCAC
<i>H-ACTA2 (<math>\alpha</math>-SMA)</i>	CTATGAGGGCTATGCTTGCC	GCTCAGCAGTAGTAACGAAGGA
<i>H-COL1A1 (Col-1)</i>	GCAAGAACCCCGCCGCACC	GCTCTCGCCGAACCAGACATGCC
<i>H-FN</i>	ATTCACCTACAATGGCAGGACGTT	GCACCAAAGATGTCCTGCTGT
<i>H-<math>\beta</math>-actin</i>	ACCCTGAAGTACCCCATCGAG	AGCACAGCCTGGATAGCAAC

**Table 2.** Antibodies used in the study

Indicator	Dilution	Origin	Cat. No. and manufacturer
HSP90α	1: 1,000	mouse	ab128483; Abcam
HSP90β	1: 5,000	rabbit	ab203085; Abcam
α-SMA	1: 2,000	rabbit	55135-1-AP; Proteintech
Col-1	1: 2,000	rabbit	14695-1-AP; Proteintech
FN	1: 5,000	rabbit	15613-1-AP; Proteintech
TGF-βRI	1: 1,000	rabbit	ab235578; Abcam
TGF-βRII	1: 1,000	rabbit	ab259360; Abcam
p-Smad2	1: 5,000	rabbit	ab188334; Abcam
Smad2	1: 6,000	rabbit	12570-1-AP; Proteintech
p-Smad3	1: 2,000	rabbit	ab52903; Abcam
Smad3	1: 3,000	mouse	66516-1-Ig; Proteintech
β-actin	1: 5,000	mouse	66009-1-Ig; Proteintech
HRP goat anti-mouse IgG	1: 5,000	mouse	SA00001-1; Proteintech
HRP goat anti-rabbit IgG	1: 6,000	rabbit	SA00001-2; Proteintech

TGF-βRI and TGF-βRII – transforming growth factor beta type receptor I and II; FN – fibronectin; HRP – horseradish peroxidase; IgG – immunoglobulin G; Col-1 – collagen 1; α-SMA – alpha-smooth muscle actin.

primary antibody at 4°C overnight. After washing with Tris-buffered saline with Tween (TBST), the membrane was mixed with the secondary antibody for 90 min. Finally, the membrane was exposed to Enhanced Chemiluminescence (ECL) Plus (AWB0005; Abiowell), and the protein bands were visualized using a gel imaging system (ChemiScope6100; Clinx, Shanghai, China). Antibody information is shown in Table 2.

## Cell culture

Human lung fibroblast 1 (HLF1) was ordered from Pricella (Wuhan, China). Cells were maintained in Ham's F-12K medium containing 10% fetal bovine serum (FBS) and 1% penicillin and streptomycin. To explore the effects of EQ in vitro, 3 groups were set up ( $n = 6$  in each group): control, TGF-β1 and TGF-β1+EQ. Cells were exposed to 10 ng/mL TGF-β1 for 48 h,<sup>37</sup> and treated with different concentrations (0, 1, 2, 4, 6, 8, and 10 μg/mL) of EQ for 48 h.

## Cell counting kit

The toxic response of EQ to HLF1 cells was tested using a Cell Counting Kit-8 (CCK-8) assay.  $5 \times 10^3$  cells were seeded in 96-well plates. After the cells adhered to the wall, 10 μL of CCK-8 solution was added to each well. After incubation at 37°C for 4 h, the absorbance of the samples was measured at 450 nm.

## Immunofluorescence

Expression of α-SMA in HLF1 cells was evaluated using an immunofluorescence (IF) assay. Cells were fixed with 4% paraformaldehyde and washed with PBS, incubated

with 0.3% Triton X-100 for 30 min, washed with PBS, then thoroughly mixed with 5% BSA for 1 h and washed with PBS. Antibody α-SMA (1:50, BM0002; Boster) was added and incubated overnight at 4°C. Then, the anti-mouse secondary antibody (1:200, AWS0004b; Abiowell) was added and incubated at 37°C for 90 min. DAPI (4',6-diamidino-2-phenylindole) was applied to stain the nucleus for 10 min. Finally, images were acquired (×400 magnification) using fluorescence microscopy (BA410E; Motic) and photographed.

## Statistical analyses

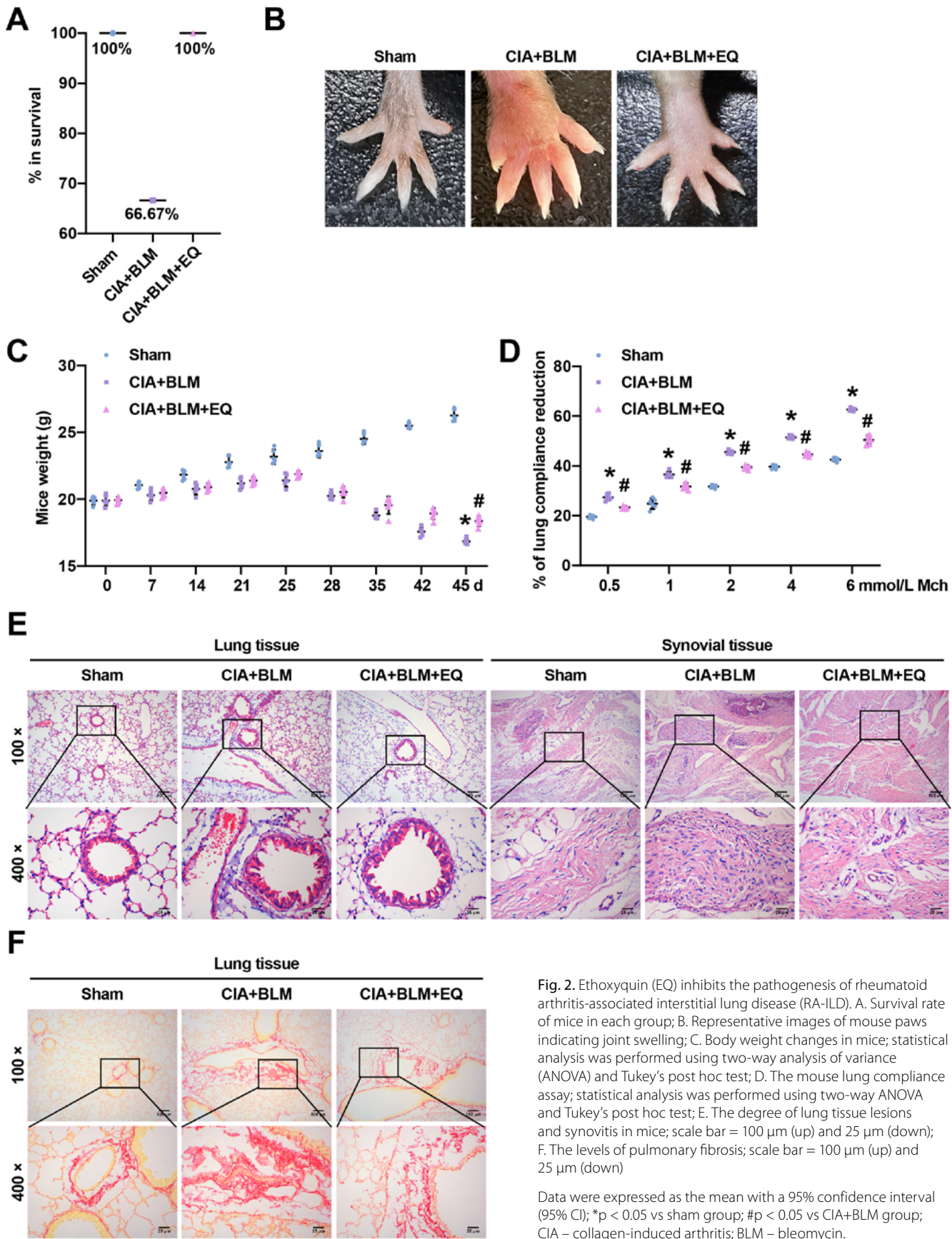
GraphPad Prism v. 9 (GraphPad Software, San Diego, USA) was used for statistical analysis. Data were expressed as the mean with a 95% confidence interval (95% CI). Normal distribution was assessed using the Shapiro–Wilk test, and the Brown–Forsythe test was used to confirm variance homogeneity (Supplementary Tables 1–6). One-way analysis of variance (ANOVA) and two-way ANOVA were used to compare groups. Tukey's post hoc test was adopted. All experiments consisted of 6 biological replicates, each representing the average of 3 technical replicates. The threshold for statistical significance was set at  $p < 0.05$ .

## Results

### Effects of EQ on disease manifestations in BLM-CIA mice

A mouse model of BLM-CIA was established to investigate the impact of EQ on RA-ILD. All the mice in the sham group survived during modeling. The CIA+BLM group





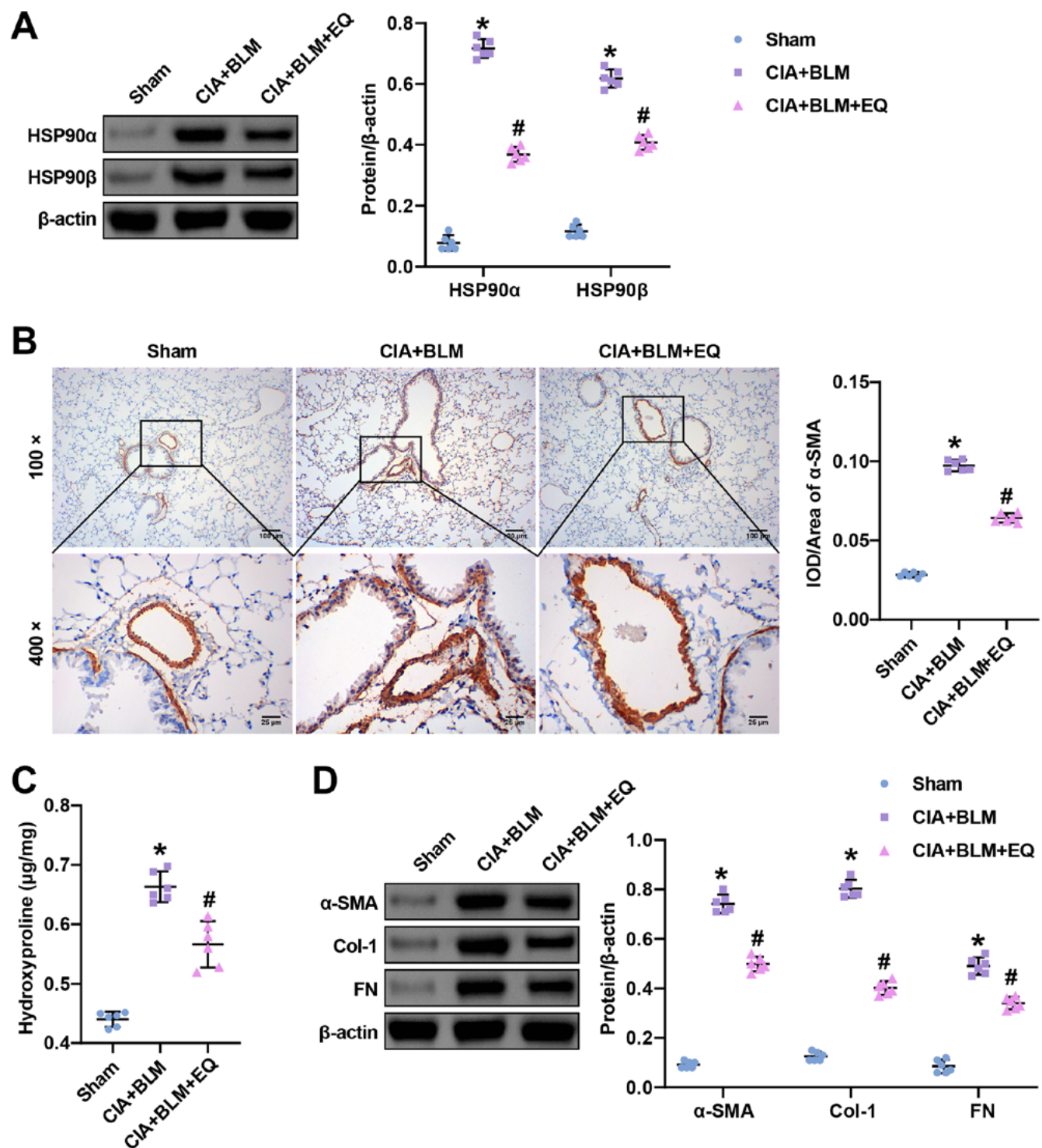


**Fig. 3.** Ethoxyquin (EQ) regulates HSP90 expression and collagen deposition in BLM-CIA mice. **A.** The abundance of HSP90α and HSP90β; **B.** The evaluation of alpha-smooth muscle actin (α-SMA) expression; scale bar = 100 μm (up) and 25 μm (down); **C.** Detection of hydroxyproline content in lung tissue; **D.** Analysis of the protein abundance of α-SMA, collagen I (Col-1) and fibronectin (FN)

Statistical analysis was performed using one-way analysis of variance (ANOVA) and Tukey's post hoc test. Data were expressed as the mean with a 95% confidence interval (95% CI); \* $p < 0.05$  vs sham group; # $p < 0.05$  vs CIA+BLM group; CIA – collagen-induced arthritis; BLM – bleomycin.

exhibited a decreased survival rate; however, treatment with EQ restored the survival rate of the diseased mice (Fig. 2A). The CIA+BLM group displayed evident redness and swelling in the paws, while EQ treatment ameliorated arthritis and swelling in the affected mice (Fig. 2B).

The body weight of the diseased mice decreased, while EQ partially restored their body weight on day 45 ( $p < 0.001$ , ANOVA, Fig. 2C). Moreover, the CIA+BLM group exhibited an increase in lung compliance reduction percentage compared to the sham group, indicating an exacerbated



reduction in lung compliance and restricted lung function in the CIA+BLM group. However, the CIA+BLM+EQ group showed a lower percentage than the CIA+BLM group ( $p < 0.001$ , ANOVA, Fig. 2D), suggesting that EQ increased lung compliance and was protective in the BLM-CIA mice. The CIA+BLM group exhibited a widened pulmonary septum, increased infiltration of macrophages and lymphocytes, elevated number of neutrophils, significant destruction of alveolar structure, and obvious inflammation. However, the severity of lung tissue lesions was notably reduced in the CIA+BLM+EQ group (Fig. 2E). In addition, H&E staining demonstrated marked joint synovial hyperplasia and infiltration of inflammatory cells in the CIA+BLM group, both of which were alleviated after EQ treatment (Fig. 2E). The CIA+BLM group mice showed significant collagen deposition in the lung interstitium, while EQ treatment alleviated this pathological phenomenon (Fig. 2F). Collectively, these results indicate that the BLM-CIA mice exhibited synovitis and pulmonary fibrosis, and treatment with EQ alleviated the physiological and pathological phenotypes associated with RA-ILD.

### Effects of EQ on HSP90 expression and collagen deposition in BLM-CIA mice

Subsequently, compared with the sham group, we found that the expression of HSP90 $\alpha$  and HSP90 $\beta$  was up-regulated in the CIA+BLM group, while EQ decreased HSP90 $\alpha$  and HSP90 $\beta$  levels ( $p < 0.001$ , ANOVA, Fig. 3A). The expression of  $\alpha$ -SMA was elevated in BLM-CIA mice, while EQ inhibited its expression ( $p < 0.001$ , ANOVA, Fig. 3B). The hydroxyproline content in the lung tissues was increased in the CIA+BLM group, which was further suppressed by EQ ( $p < 0.001$ , ANOVA, Fig. 3C). The protein abundance of  $\alpha$ -SMA, collagen I (Col-1) and fibronectin (FN) increased in the CIA+BLM group, but EQ downregulated the expression of these proteins ( $p < 0.001$ , ANOVA, Fig. 3D). Our data suggest that EQ blocked the expression of HSP90,  $\alpha$ -SMA, Col-1, and FN in BLM-CIA mice.

### Ethoxyquin affected the cellular immune status in the peripheral blood of BLM-CIA mice

Compared with the sham group, the CIA+BLM group exhibited a decrease in the proportion of M1 macrophages and an increase in M2 macrophages. Compared with the CIA+BLM group, EQ increased M1 macrophages and decreased M2 macrophages ( $p < 0.001$ , ANOVA, Fig. 4A). In the peripheral blood of the CIA+BLM group, iNOS and TNF- $\alpha$  levels were decreased, while the levels of VEGF-A and TGF- $\beta$ 1 increased. Treatment with EQ reversed these changes ( $p < 0.001$ , ANOVA, Fig. 4B). In addition, the CIA+BLM group exhibited a decrease in the proportion of Th1 and Treg cells and an increase in Th17

cells. However, EQ increased Th1 and Treg cells and decreased Th17 cells compared with the CIA+BLM group ( $p < 0.001$ , ANOVA, Fig. 4C). The level of IL-17A was increased in the CIA+BLM group, while the levels of IFN- $\gamma$  and Foxp3 were decreased. The EQ treatment reversed these changes ( $p < 0.001$ , ANOVA, Fig. 4D). These results show that in the peripheral blood of BLM-CIA mice, EQ increased M1 macrophages, Th1 and Treg subsets and decreased M2 macrophages and Th17 cells.

### Ethoxyquin regulated the cellular immune status in the lung of BLM-CIA mice

Compared with the sham group, the CIA+BLM group exhibited a decrease in the proportion of M1 macrophages and an increase in M2 macrophages in the BALF. Compared with the CIA+BLM group, EQ treatment increased M1 macrophages and decreased the M2 phenotype ( $p < 0.001$ , ANOVA, Fig. 5A). The CIA+BLM group showed reduced iNOS and TNF- $\alpha$  levels and elevated VEGF-A and TGF- $\beta$ 1 levels, while EQ reversed the levels of these factors ( $p < 0.001$ , ANOVA, Fig. 5B). In addition, the proportion of Th1 cells in the CIA+BLM group was lower, and the proportion of Th1 cells in the CIA+BLM+EQ group was higher than that of the CIA+BLM group ( $p < 0.001$ , ANOVA, Fig. 5C). The levels of IFN- $\gamma$  and Foxp3 were decreased, and IL-17A was increased in the CIA+BLM group, while EQ reversed these changes ( $p < 0.001$ , ANOVA, Fig. 5D). These results showed that EQ increased M1 macrophages and Th1 cells and decreased M2 macrophages in the lungs of BLM-CIA mice.

### Effects of EQ on the TGF- $\beta$ /Smad2/3 signaling pathway in BLM-CIA mice

We further investigated the effects of the TGF- $\beta$ /Smad2/3 pathway on RA-ILD regulated by EQ. The CIA+BLM group exhibited increased TGF- $\beta$ R, Smad2 and Smad3 mRNA levels in lung tissue, while EQ inhibited the increase of these factors ( $p < 0.001$ , ANOVA, Fig. 6A). The protein abundance of transforming growth factor beta type receptor I and II (TGF- $\beta$ RI and TGF- $\beta$ RII) was elevated in the CIA+BLM group, and EQ reversed these proteins' expression ( $p < 0.001$ , ANOVA). In addition, the ratios of p-Smad2/Smad2 and p-Smad3/Smad3 were increased in the CIA+BLM group, and EQ reversed these trends ( $p < 0.001$ , ANOVA, Fig. 6B). These data show that EQ inhibited the TGF- $\beta$ /Smad2/3 pathway in BLM-CIA mice.

### Ethoxyquin affected fibrosis-related protein expression through TGF- $\beta$ /Smad2/3 pathway in vitro

Through in vitro experiments, the role of EQ was confirmed using TGF- $\beta$ 1-induced HLF1 cells. The toxic response of different concentrations of EQ (0, 1, 2, 4, 6, 8,



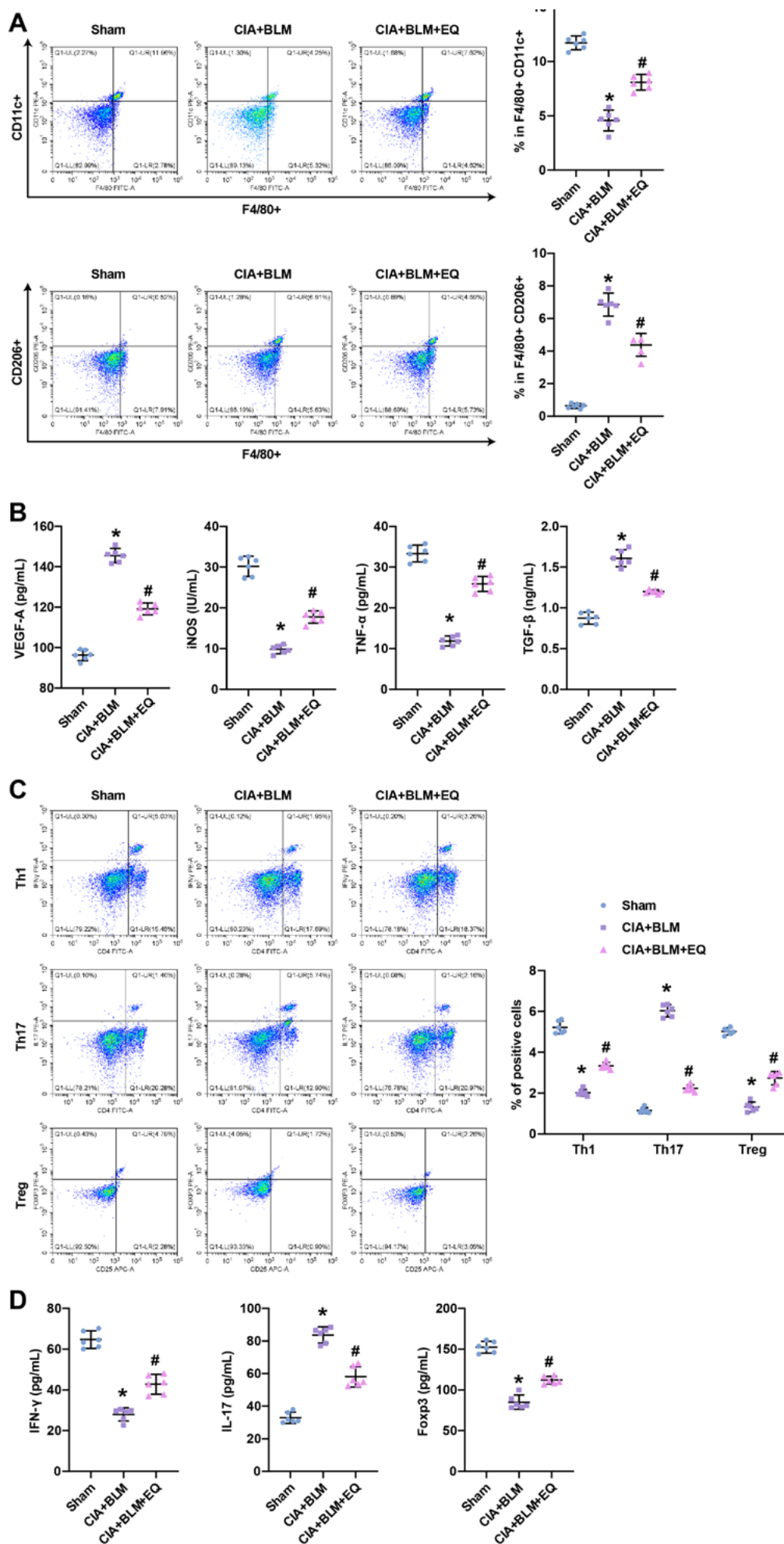


**Fig. 4.** Ethoxyquin (EQ) participates in rheumatoid arthritis-associated interstitial lung disease (RA-ILD) by regulating the proportion of immune cells in peripheral blood. **A.** The analysis of M1/M2 macrophages by F4/80<sup>+</sup> and CD11c<sup>+</sup>/CD206<sup>+</sup> double staining; **B.** The detected inducible nitric oxide synthase (iNOS) tumor growth factor alpha (TNF- $\alpha$ ), vascular endothelial growth factor (VEGF)-A, and transforming growth factor beta 1 (TGF- $\beta$ 1); **C.** Analysis of Th1, Th17 and Treg cell ratios; **D.** Detection of interferon gamma (IFN- $\gamma$ ), interleukin (IL)-17A and Foxp3

Statistical analysis was performed using one-way analysis of variance (ANOVA) and Tukey's post hoc test. Data were expressed as the mean with a 95% confidence interval (95% CI); \* $p < 0.05$  vs sham group, # $p < 0.05$  vs CIA+BLM group; CIA – collagen-induced arthritis; BLM – bleomycin.

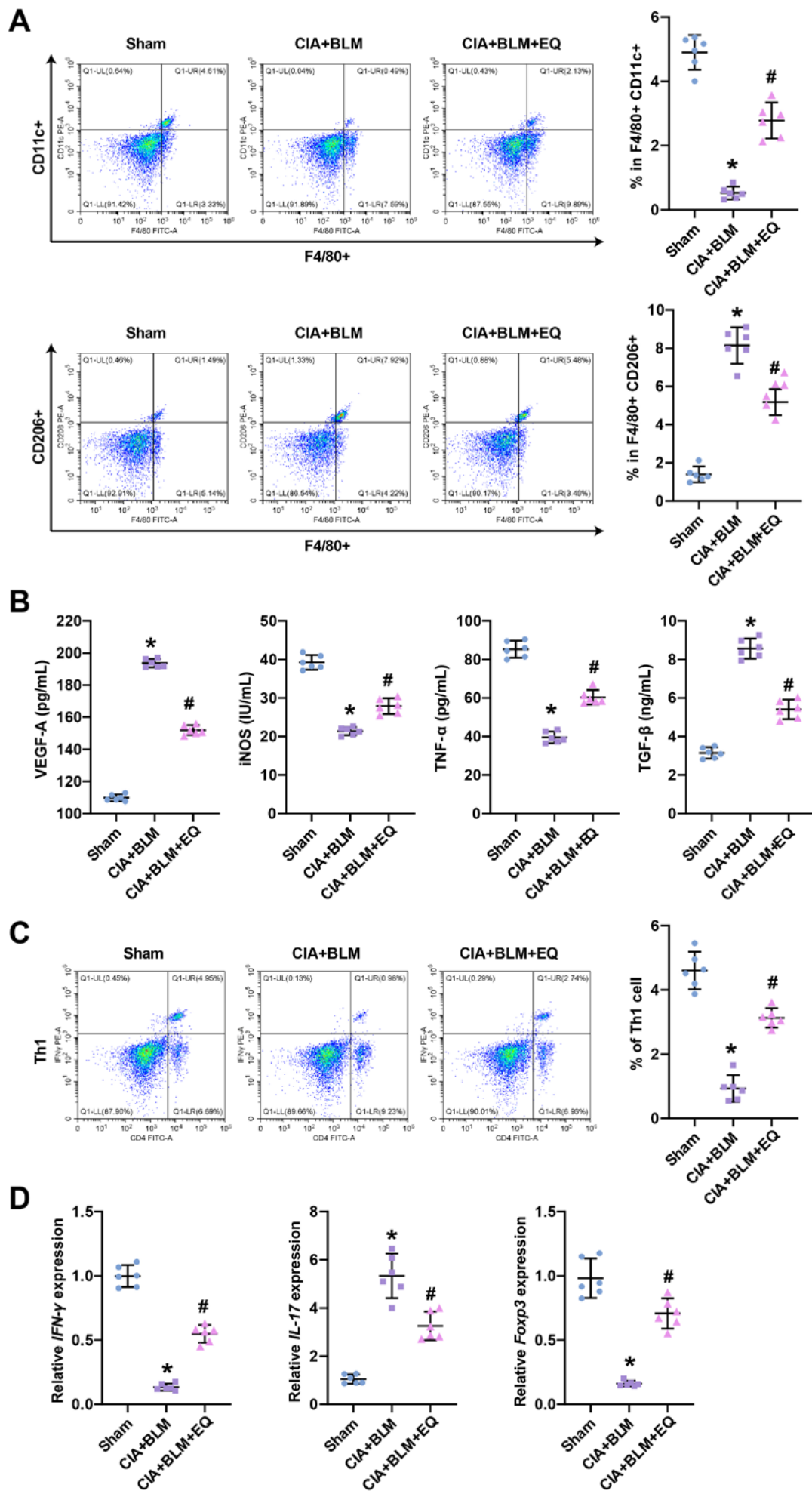
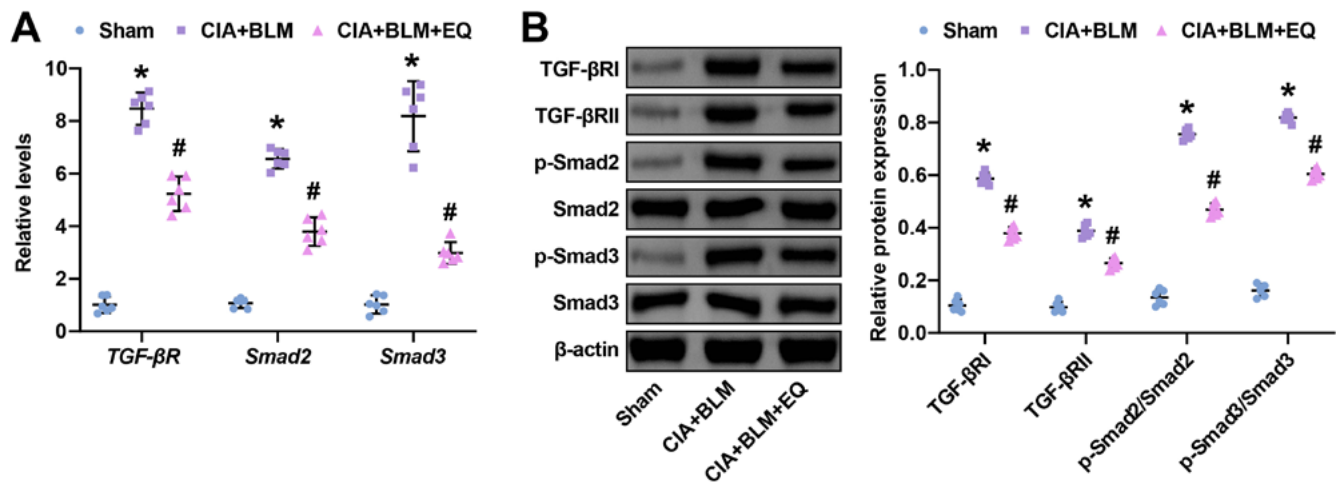


Fig. 5. Ethoxyquin (EQ) regulates the proportion of immune cells in the lungs of BLM-CIA mice. A. The analysis of M1/M2 macrophages by F4/80<sup>+</sup> and CD11c<sup>+</sup>/CD206<sup>+</sup> double staining; B. The detected inducible nitric oxide synthase (iNOS), tumor necrosis factor alpha (TNF- $\alpha$ ), vascular endothelial growth factor (VEGF-A), and transforming growth factor beta 1 (TGF- $\beta$ 1) in bronchoalveolar lavage fluid (BALF); C. The proportion of Th1 cells in BALF; D. Detection of the relative mRNA levels of interferon gamma (*IFN- $\gamma$* ), interleukin (*IL*)-17A and *Foxp3* in lung tissue homogenates

Statistical analysis was performed using one-way analysis of variance (ANOVA) and Tukey's post hoc test. Data were expressed as the mean with a 95% confidence interval (95% CI); \* $p < 0.05$  vs sham group; # $p < 0.05$  vs CIA+BLM group; CIA – collagen-induced arthritis; BLM – bleomycin.



**Fig. 6.** Ethoxyquin (EQ) blocks TGF- $\beta$ /Smad2/3 signaling to mediate the pathogenesis of rheumatoid arthritis-associated interstitial lung disease (RA-ILD). A. The relative levels of TGF- $\beta$ R and Smad2 and Smad3; B. The abundance of transforming growth factor beta type receptor I and II (TGF- $\beta$ RI and TGF- $\beta$ RII) p-Smad2, Smad2, p-Smad3, and Smad3 in lung tissue

Statistical analysis was performed using one-way analysis of variance (ANOVA) and Tukey's post hoc test. Data were expressed as the mean with a 95% confidence interval (95% CI); \* $p < 0.05$  vs sham group; # $p < 0.05$  vs CIA+BLM group; CIA – collagen-induced arthritis; BLM – bleomycin.

and 10  $\mu\text{g/mL}$ ) to HLF1 cells was evaluated. Cell Counting Kit-8 assay revealed that there were no significant differences in the viability of HLF1 cells with an increase in EQ concentration compared with the control group, suggesting that EQ had no obvious toxic effect on HLF1 cells ( $p = 0.088$ , ANOVA, Fig. 7A). Therefore, 10  $\mu\text{g/mL}$  EQ was chosen in subsequent experiments. Transforming growth factor beta 1 increased the expression of  $\alpha$ -SMA, Col-1 and FN in HLF1 cells, while EQ treatment reversed these changes ( $p < 0.001$ , ANOVA, Fig. 7B and 7C). Ethoxyquin suppressed TGF- $\beta$ 1-induced expression of  $\alpha$ -SMA in HLF1 cells ( $p < 0.001$ , ANOVA, Fig. 7D). These results demonstrate that EQ reduced EMT-specific protein expression in TGF- $\beta$ 1-exposed HLF1 cells. In addition, TGF- $\beta$ 1 promoted the expression of HSP90 $\alpha$  and HSP90 $\beta$  and increased the ratios of p-Smad2/Smad2 and p-Smad3/Smad3 in HLF1 cells, and EQ reversed the trends observed for these proteins ( $p < 0.001$ , ANOVA, Fig. 7E). These results suggest that EQ attenuated TGF- $\beta$ 1-induced expression of fibrosis-related factors in HLF1 cells.

## Discussion

Interstitial lung disease is the most important comorbidity in RA, but there is still a lack of specific treatment strategies for RA-ILD.<sup>38,39</sup> Therefore, finding therapeutics that target pulmonary fibrosis and the adaptive immune response is critical. In this study, we investigated whether the HSP90 inhibitor EQ regulates BLM-induced pulmonary fibrosis in CIA mice. The results showed that EQ restricted the protein expression of HSP90 isoforms (HSP90 $\alpha$  and HSP90 $\beta$ ). Ethoxyquin ameliorated RA-associated pathological phenotypes, namely joint swelling and synovitis, in the BLM-CIA mice. Airway responsiveness

can be used to reflect airway inflammation.<sup>40,41</sup> Pulmonary involvement in RA can cause airway impairment,<sup>42</sup> and pulmonary fibrosis also involves airway abnormalities and functional changes.<sup>43</sup> Fibrosis leads to a decrease in lung compliance, which in turn causes a decline in lung function.<sup>44,45</sup> Ethoxyquin reversed the reduction in lung compliance in BLM-CIA mice, as well as attenuated collagen deposition in the lungs of the BLM-CIA mice, as determined using H&E staining and Sirius staining. These results provide the first experimental evidence that HSP90 deficiency alleviated disease symptoms in BLM-CIA mice, thus providing novel insights and directions for the future treatment of RA-ILD.

The main pathology of pulmonary fibrosis involves the recruitment of inflammatory cells and the proliferation of lung fibroblasts, which leads to excessive deposition of ECM, mainly composed of collagen.<sup>46</sup> Col-1 is the major form of collagen in the ECM, and myofibroblasts expressing  $\alpha$ -SMA are the major source of Col-1. In our study, we observed that EQ downregulated BLM-induced  $\alpha$ -SMA expression and decreased the levels of collagen-related markers Col-1 and FN, as well as the collagen component hydroxyproline. These results confirm that EQ attenuated pulmonary fibrosis in BLM-CIA mice.

Transforming growth factor beta 1 occupies a central position in the pathogenesis of idiopathic pulmonary fibrosis (IPF). It promotes the transformation of fibroblasts into myofibroblasts and the EMT and accelerates collagen formation.<sup>34</sup> At present, evidence that the classic TGF- $\beta$ 1/Smad2/3 pathway is involved in idiopathic pulmonary fibrosis has gradually increased.<sup>47,48</sup> In our report, EQ inhibited the expression of the TGF- $\beta$  receptors TGF- $\beta$ RI and TGF- $\beta$ RII, and hindered the phosphorylation of Smad2 and Smad3. Previous reports have supported that HSP90 can stabilize TGF- $\beta$  receptors and Smads and that inhibition

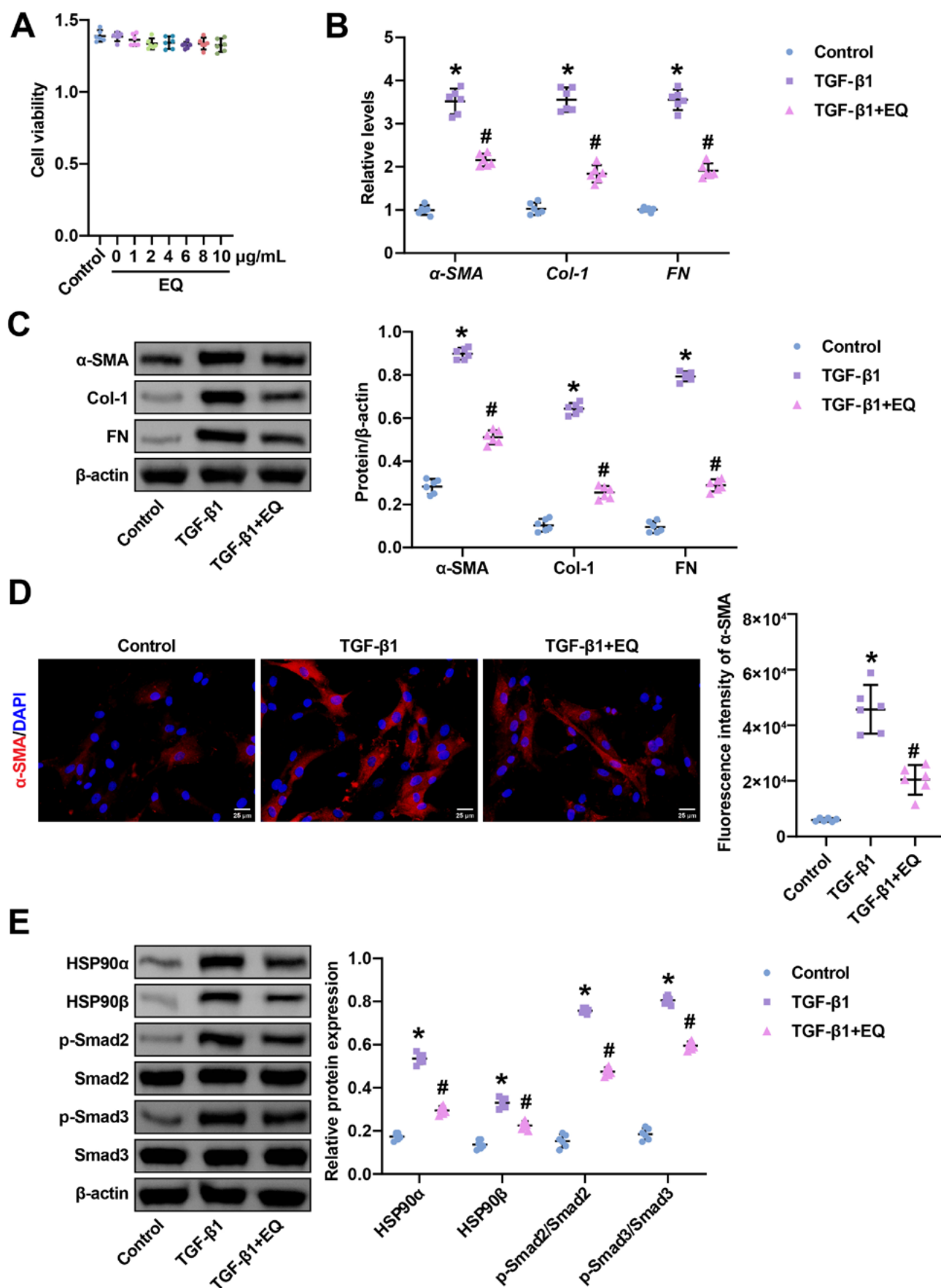


Fig. 7. Ethoxyquin (EQ) regulates the progression of rheumatoid arthritis-associated interstitial lung disease (RA-ILD) through the transforming growth factor beta (TGF- $\beta$ )/Smad2/3 pathway in vitro. A. The analysis of HLF1 cells in response to EQ cytotoxicity; B. Relative mRNA levels of alpha-smooth muscle actin ( $\alpha$ -SMA), collagen I (Col-1) and fibronectin (FN) in cells; C. Relative protein levels of  $\alpha$ -SMA, Col-1 and FN in cells; D. Assessment of  $\alpha$ -SMA expression is shown; scale bar = 25  $\mu\text{m}$ ; E. The abundance of HSP90 $\alpha$ , HSP90 $\beta$ , p-Smad2, Smad2, p-Smad3, and Smad3 in cells

Statistical analysis was performed using one-way analysis of variance (ANOVA) and Tukey's post hoc test. Data were expressed as the mean with a 95% confidence interval (95% CI); \*p < 0.05 vs control group; # p < 0.05 vs TGF- $\beta$ 1 group.



of HSP90 attenuated TGF- $\beta$ -driven myofibroblast transformation and EMT deposition.<sup>49,50</sup> We found that EQ suppressed TGF- $\beta$ 1-induced expression of  $\alpha$ -SMA, Col-1 and FN in HLF1 cells. Taken together, our data reveal that EQ alleviated pulmonary fibrosis in RA-ILD by impeding the TGF- $\beta$ 1/Smad2/3 pathway.

The number and phenotype of macrophages are critical to the fibrotic process, and induction of M2 macrophage polarization aggravates the development of pulmonary fibrosis.<sup>51</sup> Studies have shown that MBD2 stimulates PI3K/Akt signaling to enhance the macrophage M2 phenotype, and MBD2 knockdown protects BLM-induced lung fibrosis by depleting M2 macrophages.<sup>52</sup> The M2 macrophage-derived microRNAs (miRNAs) are thought to promote lung fibrosis.<sup>53</sup> Furthermore, M2 macrophages are the main source of TGF- $\beta$ 1, which induces fibroblast differentiation and proliferation.<sup>54</sup> Based on the above data, we hypothesized that EQ might impair macrophage M2 polarization to protect CIA mice from BLM-induced pulmonary fibrosis. As expected, we observed that EQ increased the proportion of M1 macrophages and decreased M2 in peripheral blood and BALF, promoting the switch of macrophages from an M2 to an M1 phenotype. Examination of the levels of markers associated with M1 and M2 macrophages supported this finding. In BLM-CIA mice, EQ upregulated iNOS and TNF- $\alpha$  and downregulated VEGF-A and TGF- $\beta$ 1.

In this study, we also found an imbalance in the T cell subsets in BLM-CIA mice. The BLM increased Th1 cells (IFN- $\gamma$ ) and Treg cells (Foxp3) and decreased Th17 cells (IL-17A) in peripheral blood and BALF. Ethoxyquin reversed the effect of BLM on Th1/Th17/Treg cells in BLM-CIA mice. T cells are key players in pulmonary fibrosis.<sup>55</sup> An increase in the ratio of Th1/Th2 cells is widely thought to exert an anti-fibrotic effect.<sup>56,57</sup> Recent evidence supports the pro-fibrotic role of Th17 cells, and inhibition of Th17 production can prevent BLM-induced pulmonary fibrosis.<sup>58,59</sup> Tregs seem to have a dual role in pulmonary fibrosis, which may be related to different models and different stages of pulmonary fibrosis.<sup>60</sup> In addition, TGF- $\beta$ 1 is very important for T cell response in pulmonary fibrosis,<sup>61,62</sup> but whether EQ mediates T cell differentiation and functional maintenance in RA-ILD through the TGF- $\beta$ 1/Smad2/3 pathway needs further evidentiary support.

## Limitations

There are some limitations to this study. A constrained timeframe and financial constraints prevented the application of TGF- $\beta$ 1 in an animal model to explore the potential involvement of the TGF- $\beta$ 1/Smad2/3 pathway in the function of EQ. Different animal models could produce varying outcomes, and further analysis is required to understand the inhibitory effects of EQ on HSP90 fully. The inability to examine the efficacy and safety of EQ in therapeutic animal models is also a limitation of this study. It should

be noted that the results from the BLM-CIA mouse model and the TGF- $\beta$ 1-induced HLF1 cell model may not necessarily reflect the same effects of EQ in human RA-ILD, and further validation in clinical samples is required. The role of the airway responsiveness test in assessing the development of RA-ILD is limited. Therefore, additional evidence is still needed to fully evaluate the effect of EQ on lung function in BLM-CIA mice. The association between RA-ILD and RA-airway diseases is worth exploring. The optimal administration route and dosage of EQ for BLM-induced CIA mice still needs to be determined. Moreover, additional research is needed to elucidate the significance of macrophage polarization and T cell responses in the development of RA-ILD, as well as to gather more evidence supporting the regulatory role of EQ on macrophage polarization and T cell responses. Sample sizes for the in vitro and in vivo experiments were also limited. We plan to utilize larger sample sizes in future studies.

## Conclusions

Our work identified EQ's previously unrecognized critical role in RA-ILD. We confirmed that EQ inhibited the TGF- $\beta$ 1/Smad2/3 pathway to attenuate synovitis, joint destruction and pulmonary fibrosis in BLM-CIA mice. Furthermore, we also illustrated that EQ promoted M2-to-M1 programming of macrophages and affected the differentiation of Th1/Th17/Treg cells. These results support the possible application of EQ as a therapy addressing the pathophysiology of RA-ILD.

## Supplementary data

The Supplementary materials are available at <https://doi.org/10.5072/zenodo.34794>. The package includes the following files:

Supplementary Table 1. Normality and uniformity test results of data and main test results in Fig. 2.

Supplementary Table 2. Normality and uniformity test results of data and main test results in Fig. 3.

Supplementary Table 3. Normality and uniformity test results of data and main test results in Fig. 4.

Supplementary Table 4. Normality and uniformity test results of data and main test results in Fig. 5.

Supplementary Table 5. Normality and uniformity test results of data and main test results in Fig. 6.

Supplementary Table 6. Normality and uniformity test results of data and main test results in Fig. 7.

## Data availability

The datasets generated and/or analyzed during the current study are available from the corresponding author on reasonable request.


## Consent for publication

Not applicable.

## ORCID iDs

Jie-Rou Huang  <https://orcid.org/0009-0000-2554-4862>

Liang Chen  <https://orcid.org/0009-0008-9868-0679>

Chao-Qian Li  <https://orcid.org/0000-0002-0916-3661>

## References

- Radu AF, Bungau SG. Management of rheumatoid arthritis: An overview. *Cells*. 2021;10(11):2857. doi:10.3390/cells10112857
- Dai Y, Wang W, Yu Y, Hu S. Rheumatoid arthritis-associated interstitial lung disease: An overview of epidemiology, pathogenesis and management. *Clin Rheumatol*. 2021;40(4):1211–1220. doi:10.1007/s10067-020-05320-z
- Cassone G, Manfredi A, Vacchi C, et al. Treatment of rheumatoid arthritis-associated interstitial lung disease: Lights and shadows. *J Clin Med*. 2020;9(4):1082. doi:10.3390/jcm9041082
- England BR, Hershberger D. Management issues in rheumatoid arthritis-associated interstitial lung disease. *Curr Opin Rheumatol*. 2020;32(3):255–263. doi:10.1097/BOR.0000000000000703
- Ba X, Wang H, Huang Y, et al. Simiao pill attenuates collagen-induced arthritis and bleomycin-induced pulmonary fibrosis in mice by suppressing the JAK2/STAT3 and TGF- $\beta$ /Smad2/3 signalling pathway. *J Ethnopharmacol*. 2023;309:116274. doi:10.1016/j.jep.2023.116274
- Kadura S, Raghu G. Rheumatoid arthritis-interstitial lung disease: Manifestations and current concepts in pathogenesis and management. *Eur Respir Rev*. 2021;30(160):210011. doi:10.1183/16000617.0011-2021
- Liang M, Matteson EL, Abril A, Distler JHW. The role of antifibrotics in the treatment of rheumatoid arthritis-associated interstitial lung disease. *Ther Adv Musculoskelet Dis*. 2022;14:1759720X2210744. doi:10.1177/1759720X221074457
- Zhang M, Zhang S. T cells in fibrosis and fibrotic diseases. *Front Immunol*. 2020;11:1142. doi:10.3389/fimmu.2020.01142
- Ubietta K, Thomas MJ, Wollin L. The effect of nintedanib on T-cell activation, subsets and functions. *Drug Des Devel Ther*. 2021;15:997–1011. doi:10.2147/DDDT.S288369
- Zhang J, Wang D, Wang L, et al. Profibrotic effect of IL-17A and elevated IL-17RA in idiopathic pulmonary fibrosis and rheumatoid arthritis-associated lung disease support a direct role for IL-17A/IL-17RA in human fibrotic interstitial lung disease. *Am J Physiol Lung Cell Mol Physiol*. 2019;316(3):L487–L497. doi:10.1152/ajplung.00301.2018
- Orecchioni M, Ghosheh Y, Pramod AB, Ley K. Macrophage polarization: Different gene signatures in M1(LPS+) vs. classically and M2(LPS-) vs. alternatively activated macrophages. *Front Immunol*. 2019;10:1084. doi:10.3389/fimmu.2019.01084
- Heukels P, Moor CC, Von Der Thüsen JH, Wijsenbeek MS, Kool M. Inflammation and immunity in IPF pathogenesis and treatment. *Respir Med*. 2019;147:79–91. doi:10.1016/j.rmed.2018.12.015
- Tang Z, Gao J, Wu J, et al. Human umbilical cord mesenchymal stromal cells attenuate pulmonary fibrosis via regulatory T cell through interaction with macrophage. *Stem Cell Res Ther*. 2021;12(1):397. doi:10.1186/s13287-021-02469-5
- Miura Y, Ohkubo H, Niimi A, Kanazawa S. Suppression of epithelial abnormalities by nintedanib in induced-rheumatoid arthritis-associated interstitial lung disease mouse model. *ERJ Open Res*. 2021;7(4):00345–02021. doi:10.1183/23120541.00345-2021
- Hoter A, El-Sabban M, Naim H. The HSP90 family: Structure, regulation, function, and implications in health and disease. *Int J Mol Sci*. 2018;19(9):2560. doi:10.3390/ijms19092560
- Colunga Biancatelli RML, Solopov P, Gregory B, Catravas JD. HSP90 inhibition and modulation of the proteome: Therapeutical implications for idiopathic pulmonary fibrosis (IPF). *Int J Mol Sci*. 2020;21(15):5286. doi:10.3390/ijms21155286
- Chen J, Song S, Liu Y, et al. Autoreactive T cells to citrullinated HSP90 are associated with interstitial lung disease in rheumatoid arthritis. *Int J Rheum Dis*. 2018;21(7):1398–1405. doi:10.1111/1756-185X.13316
- Harlow L, Gochuico BR, Rosas IO, et al. Anti-citrullinated heat shock protein 90 antibodies identified in bronchoalveolar lavage fluid are a marker of lung-specific immune responses. *Clin Immunol*. 2014;155(1):60–70. doi:10.1016/j.clim.2014.08.004
- Wang J, Mai K, Ai Q. Conventional soybean meal as fishmeal alternative in diets of Japanese seabass (*Lateolabrax japonicus*): Effects of functional additives on growth, immunity, antioxidant capacity and disease resistance. *Antioxidants*. 2022;11(5):951. doi:10.3390/antiox11050951
- Zhou HB, Huang XY, Bi Z, et al. Vitamin A with L-ascorbic acid sodium salt improves the growth performance, immune function and antioxidant capacity of weaned pigs. *Animal*. 2021;15(2):100133. doi:10.1016/j.animal.2020.100133
- Iskusnykh IY, Kryl'skii ED, Brazhnikova DA, et al. Novel antioxidant, deethylated ethoxyquin, protects against carbon tetrachloride induced hepatotoxicity in rats by inhibiting NLRP3 inflammasome activation and apoptosis. *Antioxidants*. 2021;10(1):122. doi:10.3390/antiox10010122
- Tayel F, Mahfouz ME, Salama AF, Mansour MA. Ethoxyquin inhibits the progression of murine Ehrlich ascites carcinoma through the inhibition of autophagy and LDH. *Biomedicines*. 2021;9(11):1526. doi:10.3390/biomedicines9111526
- Zhu J, Chen W, Mi R, Zhou C, Reed N, Höke A. Ethoxyquin prevents chemotherapy-induced neurotoxicity via Hsp90 modulation. *Ann Neurol*. 2013;74(6):893–904. doi:10.1002/ana.24004
- Zhu J, Carozzi VA, Reed N, et al. Ethoxyquin provides neuroprotection against cisplatin-induced neurotoxicity. *Sci Rep*. 2016;6(1):28861. doi:10.1038/srep28861
- Chen D, Tang H, Jiang H, Sun L, Zhao W, Qian F. ACPA alleviates bleomycin-induced pulmonary fibrosis by inhibiting TGF- $\beta$ -Smad2/3 signaling-mediated lung fibroblast activation. *Front Pharmacol*. 2022;13:835979. doi:10.3389/fphar.2022.835979
- Li SR, Tan ZX, Chen YH, et al. Vitamin D deficiency exacerbates bleomycin-induced pulmonary fibrosis partially through aggravating TGF- $\beta$ /Smad2/3-mediated epithelial-mesenchymal transition. *Respir Res*. 2019;20(1):266. doi:10.1186/s12931-019-1232-6
- Lee JH, Massagué J. TGF- $\beta$  in developmental and fibrogenic EMTs. *Semin Cancer Biol*. 2022;86:136–145. doi:10.1016/j.semcancer.2022.09.004
- Xu R, Wu M, Wang Y, et al. Mesenchymal stem cells reversibly differentiate myofibroblasts to fibroblast-like cells by inhibiting the TGF- $\beta$ -SMAD2/3 pathway. *Mol Med*. 2023;29(1):59. doi:10.1186/s10020-023-00630-9
- Zhang Q, Ye H, Xiang F, et al. miR-18a-5p inhibits sub-pleural pulmonary fibrosis by targeting TGF- $\beta$  receptor II. *Mol Ther*. 2017;25(3):728–738. doi:10.1016/j.ymthe.2016.12.017
- Xiong L, Xiong L, Ye H, Ma W. Animal models of rheumatoid arthritis-associated interstitial lung disease. *Immun Inflamm Dis*. 2021;9(1):37–47. doi:10.1002/iid3.377
- Hashida R, Shimozuru Y, Chang J, Agosto-Marlin I, Waritani T, Terao K. New studies of pathogenesis of rheumatoid arthritis with collagen-induced and collagen antibody-induced arthritis models: New insight involving bacteria flora. *Autoimmun Dis*. 2021;2021:7385106. doi:10.1155/2021/7385106
- Luan J, Hu Z, Cheng J, et al. Applicability and implementation of the collagen-induced arthritis mouse model, including protocols (Review). *Exp Ther Med*. 2021;22(3):939. doi:10.3892/etm.2021.10371
- Ishida Y, Kuninaka Y, Mukaida N, Kondo T. Immune mechanisms of pulmonary fibrosis with bleomycin. *Int J Mol Sci*. 2023;24(4):3149. doi:10.3390/ijms24043149
- Ye Z, Hu Y. TGF- $\beta$ 1: Gentlemanly orchestrator in idiopathic pulmonary fibrosis (Review). *Int J Mol Med*. 2021;48(1):132. doi:10.3892/ijmm.2021.4965
- Chanda D, Otoupalova E, Smith SR, Volckaert T, De Langhe SP, Thannickal VJ. Developmental pathways in the pathogenesis of lung fibrosis. *Mol Aspects Med*. 2019;65:56–69. doi:10.1016/j.mam.2018.08.004
- Tsoyi K, Esposito AJ, Sun B, et al. Syndecan-2 regulates PAD2 to exert antifibrotic effects on RA-ILD fibroblasts. *Sci Rep*. 2022;12(1):2847. doi:10.1038/s41598-022-06678-7
- Dong L, Wang Y, Zheng T, et al. Hypoxic hUCMSC-derived extracellular vesicles attenuate allergic airway inflammation and airway remodeling in chronic asthma mice. *Stem Cell Res Ther*. 2021;12(1):4. doi:10.1186/s13287-020-02072-0

38. Akiyama M, Kaneko Y. Pathogenesis, clinical features, and treatment strategy for rheumatoid arthritis-associated interstitial lung disease. *Autoimmun Rev*. 2022;21(5):103056. doi:10.1016/j.autrev.2022.103056
39. Yamakawa H, Ogura T, Kameda H, et al. Decision-making strategy for the treatment of rheumatoid arthritis-associated interstitial lung disease (RA-ILD). *J Clin Med*. 2021;10(17):3806. doi:10.3390/jcm10173806
40. Aghasafari P, George U, Pidaparti R. A review of inflammatory mechanism in airway diseases. *Inflamm Res*. 2019;68(1):59–74. doi:10.1007/s00011-018-1191-2
41. Athari SS. Targeting cell signaling in allergic asthma. *Sig Transduct Target Ther*. 2019;4(1):45. doi:10.1038/s41392-019-0079-0
42. Matson SM, Demoruelle MK, Castro M. Airway disease in rheumatoid arthritis. *Ann Am Thorac Soc*. 2022;19(3):343–352. doi:10.1513/AnnalsATS.202107-876CME
43. Chakraborty A, Mastalerz M, Ansari M, Schiller HB, Staab-Weijnitz CA. Emerging roles of airway epithelial cells in idiopathic pulmonary fibrosis. *Cells*. 2022;11(6):1050. doi:10.3390/cells11061050
44. Atsumi K, Saito Y, Tanaka T, et al. A possible, non-invasive method of measuring dynamic lung compliance in patients with interstitial lung disease using photoplethysmography. *J Nippon Med Sch*. 2021;88(4):326–334. doi:10.1272/jnms.JNMS.2021\_88-411
45. Shieh JM, Tseng HY, Jung F, Yang SH, Lin JC. Elevation of IL-6 and IL-33 levels in serum associated with lung fibrosis and skeletal muscle wasting in a bleomycin-induced lung injury mouse model. *Mediators Inflamm*. 2019;2019:7947596. doi:10.1155/2019/7947596
46. Hewlett JC, Kropski JA, Blackwell TS. Idiopathic pulmonary fibrosis: Epithelial–mesenchymal interactions and emerging therapeutic targets. *Matrix Biol*. 2018;71–72:112–127. doi:10.1016/j.matbio.2018.03.021
47. Yao Y, Yuan Y, Lu Z, et al. Effects of *Nervilia fordii* extract on pulmonary fibrosis through TGF- $\beta$ /Smad signaling pathway. *Front Pharmacol*. 2021;12:659627. doi:10.3389/fphar.2021.659627
48. Wang Y, Sun S, Wang K, et al. Interleukin-19 aggravates pulmonary fibrosis via activating fibroblast through TGF- $\beta$ /Smad pathway. *Mediators Inflamm*. 2022;2022:6755407. doi:10.1155/2022/6755407
49. Roberts RJ, Hallee L, Lam CK. The potential of Hsp90 in targeting pathological pathways in cardiac diseases. *J Pers Med*. 2021;11(12):1373. doi:10.3390/jpm11121373
50. Sontake V, Wang Y, Kasam RK, et al. Hsp90 regulation of fibroblast activation in pulmonary fibrosis. *JCI Insight*. 2017;2(4):e91454. doi:10.1172/jci.insight.91454
51. Cheng P, Li S, Chen H. Macrophages in lung injury, repair, and fibrosis. *Cells*. 2021;10(2):436. doi:10.3390/cells10020436
52. Wang Y, Zhang L, Wu GR, et al. MBD2 serves as a viable target against pulmonary fibrosis by inhibiting macrophage M2 program. *Sci Adv*. 2021;7(1):eabb6075. doi:10.1126/sciadv.abb6075
53. Kishore A, Petrek M. Roles of macrophage polarization and macrophage-derived miRNAs in pulmonary fibrosis. *Front Immunol*. 2021;12:678457. doi:10.3389/fimmu.2021.678457
54. Rao LZ, Wang Y, Zhang L, et al. IL-24 deficiency protects mice against bleomycin-induced pulmonary fibrosis by repressing IL-4-induced M2 program in macrophages. *Cell Death Differ*. 2021;28(4):1270–1283. doi:10.1038/s41418-020-00650-6
55. Kagawa K, Sato S, Koyama K, et al. The lymphocyte-specific protein tyrosine kinase-specific inhibitor A-770041 attenuates lung fibrosis via the suppression of TGF- $\beta$  production in regulatory T-cells. *PLoS One*. 2022;17(10):e0275987. doi:10.1371/journal.pone.0275987
56. Mojiri-Forushani H, Hemmati AA, Khodadadi A, Rashno M. Valsartan attenuates bleomycin-induced pulmonary fibrosis by inhibition of NF- $\kappa$ B expression and regulation of Th1/Th2 cytokines. *Immunopharmacol Immunotoxicol*. 2018;40(3):225–231. doi:10.1080/08923973.2018.1431924
57. Cao H, Zhou X, Zhang J, et al. Hydrogen sulfide protects against bleomycin-induced pulmonary fibrosis in rats by inhibiting NF- $\kappa$ B expression and regulating Th1/Th2 balance. *Toxicol Lett*. 2014;224(3):387–394. doi:10.1016/j.toxlet.2013.11.008
58. Celada LJ, Kropski JA, Herazo-Maya JD, et al. PD-1 up-regulation on CD4<sup>+</sup> T cells promotes pulmonary fibrosis through STAT3-mediated IL-17A and TGF- $\beta$ 1 production. *Sci Transl Med*. 2018;10(460):eaar8356. doi:10.1126/scitranslmed.aar8356
59. Park SJ, Hahn HJ, Oh SR, Lee HJ. Theophylline attenuates BLM-induced pulmonary fibrosis by inhibiting Th17 differentiation. *Int J Mol Sci*. 2023;24(2):1019. doi:10.3390/ijms24021019
60. Wang F, Xia H, Yao S. Regulatory T cells are a double-edged sword in pulmonary fibrosis. *Int Immunopharmacol*. 2020;84:106443. doi:10.1016/j.intimp.2020.106443
61. Kitani A, Fuss I, Nakamura K, Kumaki F, Usui T, Strober W. Transforming growth factor (TGF)- $\beta$ 1-producing regulatory T cells induce Smad-mediated interleukin 10 secretion that facilitates coordinated immunoregulatory activity and amelioration of TGF- $\beta$ 1-mediated fibrosis. *J Exp Med*. 2003;198(8):1179–1188. doi:10.1084/jem.20030917
62. Liu F, Liu J, Weng D, et al. CD4<sup>+</sup>CD25<sup>+</sup>Foxp3<sup>+</sup> regulatory T cells depletion may attenuate the development of silica-induced lung fibrosis in mice. *PLoS One*. 2010;5(11):e15404. doi:10.1371/journal.pone.0015404